Proceedings of ASME 34th International Conference on Ocean, Offshore and Arctic Engineering
OMAE 2015
May 31- June 5, St. John's, NL, Canada

OMAE2015-41386

STRUCTURAL INTEGRITY OF BUCKLED STEEL PIPES

Aglaia E. Pournara
Dept. of Mechanical Engineering
University of Thessaly, Volos, Greece
email: agpourna@gmail.com

Theocharis Papatheocharis
Dept. of Civil Engineering
University of Thessaly, Volos, Greece

Spyros A. Karamanos
Dept. of Mechanical Engineering
University of Thessaly, Volos, Greece

Philip C. Perdikaris
Dept. of Civil Engineering
University of Thessaly, Volos, Greece

ABSTRACT

Local distortions on steel pipeline wall in the form of buckles may constitute a threat for the structural integrity of the steel pipeline. In the present paper, experimental research supported by numerical simulation is reported to investigate the structural integrity of buckled steel pipes. A series of six (6) full-scale experiments has been carried out on 6-inch X52 pipes, followed by finite element simulations. The buckled steel pipes are subjected to cyclic loading (bending or pressure) in order to estimate their residual strength and remaining fatigue life. The finite element analysis simulates the experimental procedure for each type of deformation and loading case, in order to estimate the local strain distributions at the buckled region. Based on the numerical results, fatigue life is predicted and compared with the experimental results using an appropriate defined damage factor. The results of the present study are aimed at evaluating existing guidelines and methodologies towards appropriate assessment of local wall distortions in steel pipelines.

INTRODUCTION

Evaluating the severity of pipe wall distortions constitutes a crucial step towards safeguarding the structural integrity of aging hydrocarbon pipeline infrastructure [1][2]. For numerous pipeline systems that have been in service for more than four decades, monitoring and maintaining a reliable level of their operational condition has motivated significant amount of research, which is reflected in relevant standards [3] and guidelines [4].

The effect of various defects (dents, gouges, manufacturing or weld defects, corrosion) on the structural integrity of pipelines has been examined in a joint industry project based on existing experimental and numerical results [4]. Considering a large number of publications regarding the ultimate capacity or the fatigue strength of defected or damaged pipelines, this work aimed at the enhancement of the current methodologies and the identification of "gaps" in existing knowledge towards a "fitness-for-purpose" pipeline assessment.

In the event of pipe wall wrinkling, referred to as local buckling, caused during field cold bending, or permanent ground motion in geohazard areas, the pipeline may appear to fulfill its transportation function, provided that the steel material is adequately ductile and no cracks occur. However, the damaged area is associated with significant strain concentrations and, in the case of repeated loading cracks may develop, leading to fatigue failure.

On the other hand, limited information is currently available for the structural capacity of buckled pipelines, especially under cyclic bending loadings caused by temperature variations or permafrost actions. The available design standards and guidelines do address the assessment of buckles on pipe integrity. Furthermore, the criteria to determine local buckle severity have not yet been clarified.

Most of the international pipeline codes usually refer to the case of dented (gouged or non-gouged) pipelines under internal pressure variations and corrosion. Dents on pipe wall are usually non-acceptable if they exceed a depth of 6% of the nominal pipe diameter, whereas a more elaborate methodology for dent acceptability is described in Appendix R of ASME B31.8 [5] based on a calculation of maximum local strain at the dent region.

A first attempt to present an assessment procedure of buckles/wrinkles under cyclic pressure and pipe wall corrosion has been presented in [6], based on ASME B31.8 provisions [5]. According to this report, wrinkles can be acceptable for peak-to-trough heights up to 1% of the pipe diameter, as recommended in [7] for pipeline field bends.

Dama et al. [8] presented experimental and numerical research conducted to assess the structural condition of buckled pipes, subjected to both bending and internal pressure. The results of that study demonstrate that under repeated loading, fatigue failure occurs in the buckled area at the location of maximum strain range. More recently, Das et al. [9] conducted full-scale laboratory tests to investigate the post-wrinkling ultimate behavior of steel pipelines. The pipe specimens exhibited extreme ductile behavior and did not fail in fracture under monotonically increasing axisymmetric compressive axial loads and displacements. Fractures developed at the wrinkled region, however, when a wrinkled pipe specimen was subjected to cyclic strain reversals due to unloading and loading of primary loads.

The present study is part of an extensive research program conducted at the University of Thessaly on the effects of local pipe wall distortions on the structural integrity of steel pipelines. It constitutes and a continuation of the work presented in [10], where experimental and analytical work for predicting the remaining fatigue life of dented pipes has been reported. The work reported in [10] refers to dented 6-inch diameter X52 pipelines with diameter-to-thickness ratio D/t equal to 35, subjected to cyclic bending and pressure. It is found that cyclic bending on dented specimens, causes fatigue cracking, located at the ridge of the deformed area, at about 1,000 loading cycles. In addition, a finite element simulation of the experimental procedure has been performed in [10], which allows for a reliable prediction of pipeline fatigue life, based on local strain variation. For the particular case of pressure loading, the results indicated that dented pipes with dent depth larger than 12% of pipe diameter can sustain a significant number of pressure cycles.

In the present paper, experimental research is presented supported by numerical simulation, to investigate the residual structural integrity of buckled steel pipes. A first part of this work, consisting of numerical results only, was presented in [11]. In the present work, a series of six (6) full-scale experiments on ∅165/3 (6-inch-diameter, 3-mm-thick) pipes of steel grade X52 is carried out. The steel pipes are initially buckled up to different levels and, subsequently, they are subjected to further cyclic loading (bending or pressure) in order to estimate their residual strength and remaining life. Furthermore, finite element analyses are also conducted to simulate the experimental procedure for each type of deformation and loading case, and calculate strain distributions at the buckled region, so that the fatigue life of the specimen is estimated and compared with the experimental results. The results of the present study are aimed at better understanding of the mechanical behavior of locally buckled steel pipes, towards reliable assessment of local wall distortions and efficient pipeline integrity management.

SPECIMENS AND EXPERIMENTAL SET-UP

This series of tests is part of an extensive experimental investigation on 6-inch pipe specimens (according to [12]). The pipe specimens, considered in the present study, have been machined, with a lathe device, from ∅168.3/4.78 pipes in order to investigate the response of specimens with diameter to thickness ratios (D/t) larger than 30. The thickness was reduced by removing uniformly the outer steel pipe material around the pipe cross section via a cutting saddle. The 6-inch specimens' thickness was reduced to a constant mean value of 2.8mm along a 500mm-long central area. On both ends of this area, there exist two 100mm-long transition zones in which the thickness is gradually decreased from the pipe ends to the initiation of the central region. These zones have been machined with a smooth slope of less than 2^o degrees to avoid geometrical discontinuities which will affect the experimental results. Through this procedure, pipes of with nominal values of D=165mm and t= 3mm (named as ∅165/3 specimens), were produced from 6-inch pipes.

Six (6) full-scale tests are performed, consisting of cyclic loading applied on buckled ∅165/3 pipe specimens shown in Figure 1. First, the six (6) pipe specimens are buckled at zero pressure, and subsequently, they are subjected to cyclic loading as follows:

- four (4) pipes subjected to cyclic bending
- two (2) pipes subjected to cyclic pressure.

Buckling was induced through the application of monotonic four-point bending up to a certain post-buckling level. Subsequently, cyclic bending loading was applied with the same four-point bending set-up and cyclic pressure was applied with the specimen ends capped with thick plates until fatigue cracking occurs in the low-cycle fatigue range.

In the following paragraphs, the procedure of buckling, cyclic bending and pressure loading are described. Cyclic bending has been conducted at the laboratory facilities of the University of Thessaly, Department of Civil Engineering, whereas the two pressure tests have been performed at the facilities of EBETAM S.A., located in Volos, Greece.

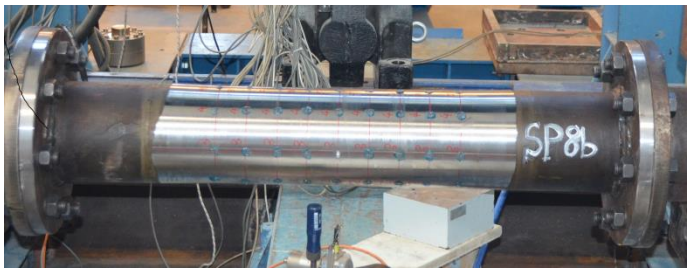

Figure 1: X52 6-inch diameter pipe specimens, machined at 2.8mm thickness.

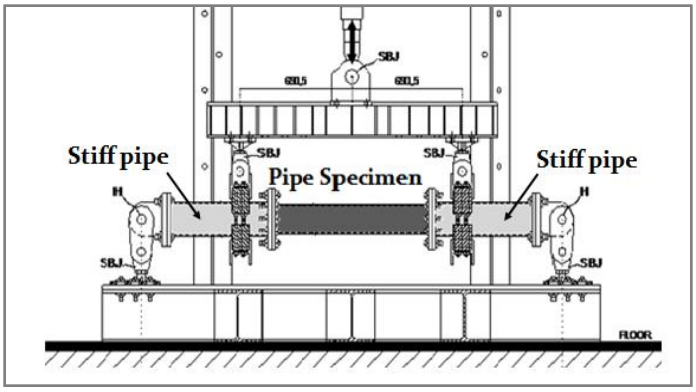

Figure 2: Schematic configuration of four-point bending set-up.

Monotonic and Cyclic bending set-up

The set-up employed for buckling development and cyclic bending on the pipe specimens is shown in Figure 2 and Figure 3. The 1-meter-long specimens are connected on either side to two heavy-walled 7-inch-diameter 650-mm-long tube segments (∅193.7/10) made of high-strength steel using a bolted connection referred to as "stiff pipe" in Figure 2. The entire system is 2.615-meters long, hinged at the two ends (Figure 4a) and connected to the 600-kN-force-capacity hydraulic actuator through a cross-beam and two wooden clamps (Figure 4b). This corresponds to a four-point bending structural system, where monotonic and cyclic bending is applied through the vertical motion of the hydraulic actuator. The hinges of this 4-point bending set-up also minimize the axial load introduced during bending, because of the end slope of the specimen axis. Local strains are measured throughout the experimental procedure through strain gauges located at several positions along the pipe specimens. Prior to cyclic loading, additional strain gauges have been implemented in the critical region of the buckle after its occurrence in order to measure local strain variations before crack initiation.

Pressure test procedure

Two (2) buckled specimens have been pressurized with the use of a 400-bar-capacity water pump (Figure 5). Cyclic pressure has been applied with maximum (P_{max}) and minimum (P_{min}) 92.9 bar and 9.2 bar, respectively, at a frequency of about 0.1 Hz. Following cyclic testing, one (1) specimen was pressurized monotonically until burst.

GEOMETRICAL AND MATERIAL PROPERTIES

Material testing

Tests for the characterization of material properties were performed on the X52 steel pipe material to determine material properties. Strip specimens have been extracted from the seamless 6-inch pipes, in the longitudinal direction and machined in accordance with the ASTM E606 standard. The material stress-strain curve was obtained from tensile coupon tests, indicating a yield stress (σ_Y) equal to 356MPa, very close to the nominal value, and an ultimate stress (σ_{UTS}) equal to 554.7 MPa at about 18% uniform elongation.

In addition to tensile testing, a total of thirty (30) cyclic tests were performed on strip specimens with loading ratio R equal to -1 and 0. In those tests, the hysteresis loops at different strain ranges were determined and the fatigue ($\Delta\varepsilon - N$) curve for the pipe X52 steel were developed. The tests have been performed in the facilities of FEUP at Porto, Portugal [13] and the corresponding fatigue curve can be expressed by the following Coffin-Manson-Basquin equation:

$$\Delta\varepsilon = 0.0102(2N)^{-0.1133} + 0.333(2N)^{-0.4807} \qquad (1)$$

Figure 3: Four-point bending experimental set-up.

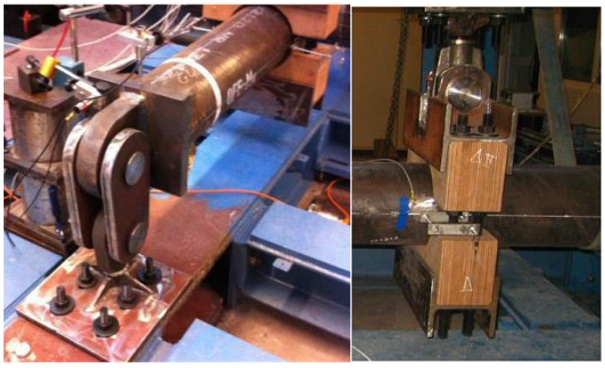
(a) (b)

Figure 4: (a) bending specimen hinges and (b) wooden clamp.


Figure 5: Pressure application on specimens.

Thickness measurements

Prior to testing the specimens, thickness measurements have been obtained using an ultrasonic device at specific points around several cross sections along the specimen's length (Figure 6). A mean thickness value has been measured equal to 2.794mm. A ∅165/3 specimen is shown in Figure 6 after marking for thickness measurements.

The geometrical properties of the specimens under consideration are summarized in Table 1. It is observed that the measurements did not show a significant variation of thickness with respect to the mean thickness values.

(a) (b)

Figure 6: (a) Thickness measurements via ultrasonic device and (b) marked ∅165/3 specimen.

Table 1. Geometrical properties of pipe specimens; nominal diameter is D_{nom}=165 mm

Specimens	t_{mean} (mm)	Type of loading
SP3b	3.268	Cyclic Bending
SP4b	2.680	
SP5b	2.747	
SP6b	2.808	
SP7b	2.895	Cyclic Pressure
SP8b	2.943	

EXPERIMENTAL RESULTS

To form a buckle on the pipe wall, the specimens are subjected to monotonic 4-point bending using the experimental set-up shown in Figure 3. Monotonic bending is applied and continued well into the post buckling regime until the desired size of buckle is developed on the compressive side of the specimen. The level of buckling is defined from the ratio of P_b/P_m, where P_b value refers to the predefined load level reached on the post buckling brunch and P_m is the maximum load sustained by the specimen. Three levels of buckle have been investigated corresponding to P_b/P_m ratios equal to 0.55, 0.65 and 0.75.

Subsequently, cyclic bending is applied to four (4) buckled specimens, while pressure loading was applied on the two (2) buckled specimens remaining. Table 2, Table 3 and Table 4 show an overview of the experimental activity.

Buckle development

Each specimen is connected to the set-up configuration shown in Figure 3 and subjected to monotonic four-point bending until the desired size of buckle is achieved. The loading sequence for SP3b-SP6b specimens during buckling development and cyclic loading are shown in Figure 7 in terms of load-stroke curves. Similarly, the load-stroke curves for SP7b and SP8b specimens during buckle development are shown in Figure 8. From these Figures, it is shown that each specimen exhibits different buckling and post-buckling behavior. This is mostly attributed to the sensitivity of buckling on thickness variation on the compression side due to machining and the presence of initial imperfections.

During monotonic bending, strain values are recorded from the strain gauges instrumented in several points and critical regions along the pipe wall (Figure 9). Furthermore, wire transducers are employed to measure movement of grips as well as the transverse displacement of the pipe central section (wires R, S and K, respectively) parallel to stroke application direction. The one end of each wire (R , S and K) was fixed to the floor and the other end was connected to each one of the two grips, for R and S, while and. the moving end of wire K was hanged by a small bolt which was drilled, sideways, in the pipe central section, as illustrated in Figure 15. The displacements measured via wire transducers are recorded and compared with the stroke applied through the machine. The wire displacement values are presented in terms of the load values measured by the actuator and compared indicatively for SP4b and SP7b specimens, as shown in Figure 10 and Figure 11.

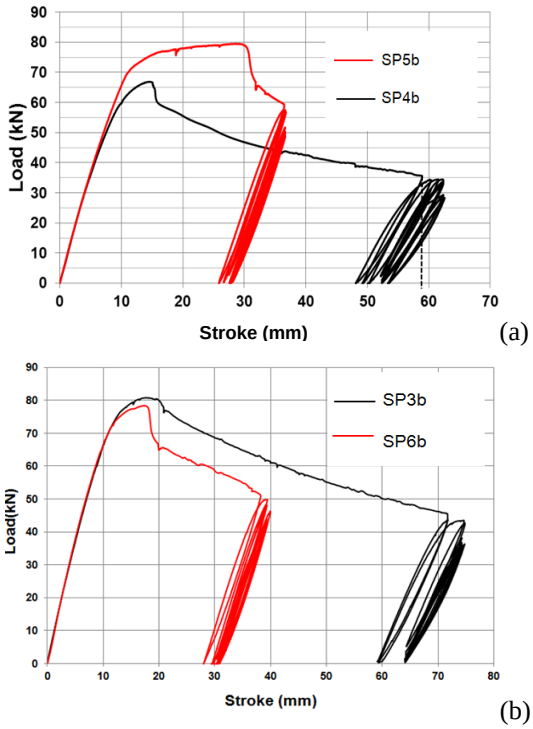

Figure 7: The loading sequence for the buckled specimens (a) SP4b & SP5b and (b) SP3b & SP6b under cyclic bending

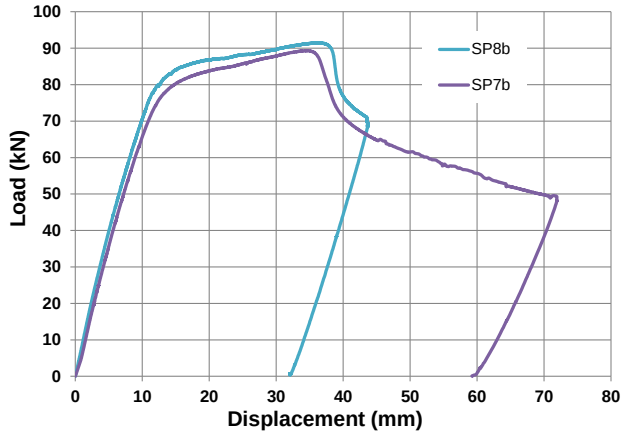

Figure 8: Buckle development of specimens SP7b and SP8b.

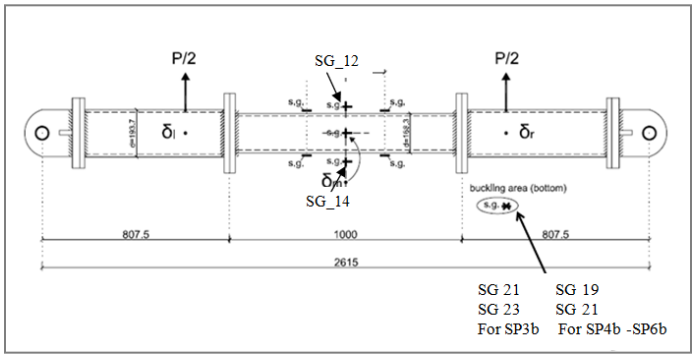

Figure 9: Strain gauges instrumentation before monotonic and cyclic bending of SP3b-SP6b specimens

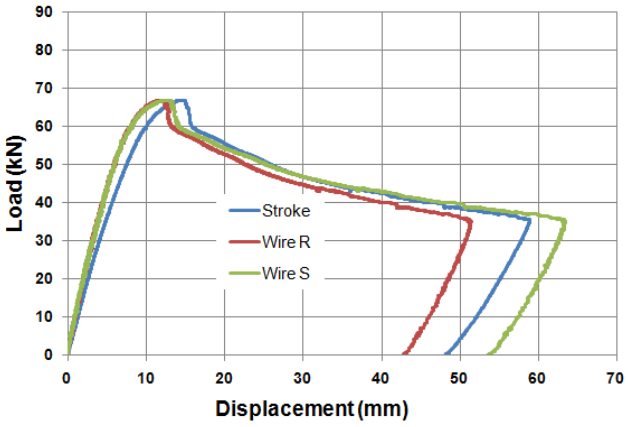

Figure 10: Load vs displacement curves during monotonic loading of SP4b specimen.

Moreover, tensile and compressive axial strain values in the central cross-section are obtained. Figure 12 shows the maximum tensile and compressive axial strain values obtained from specific points located diametrically opposite around the central cross section of the SP4b specimen during monotonic bending.

The graphs of Figure 12 show that the tensile strain values follow the trend of load-displacement curves, while the curve corresponding to the strain values in the compressive region, changes abruptly due to local buckle development of the local buckle in the compressive side and the formation of the wrinkling pattern.

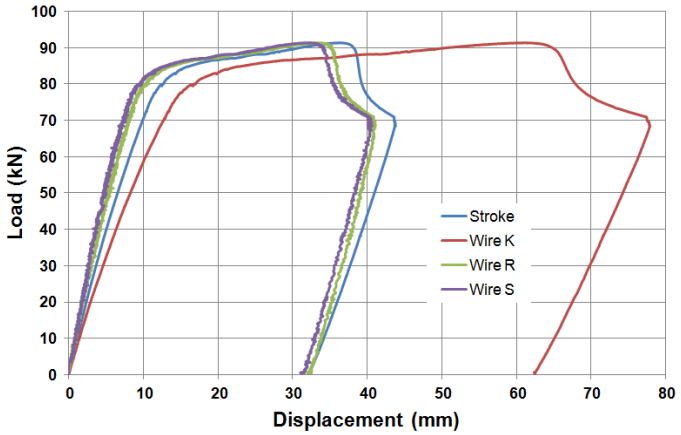

Figure 11: Load vs displacement curves during monotonic loading for SP8b specimen.

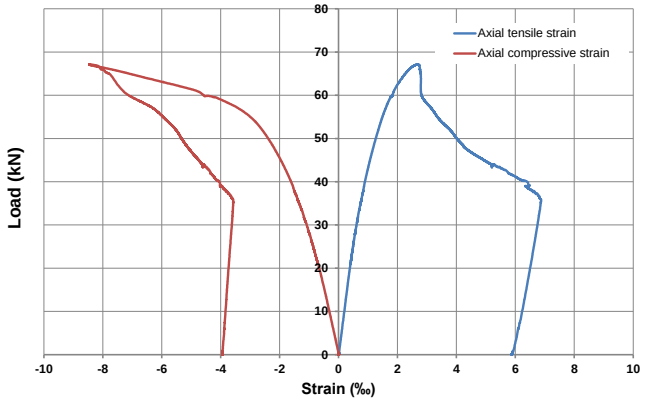

Figure 12: Strain evolution in terms of load during monotonic bending; specimen SP4b

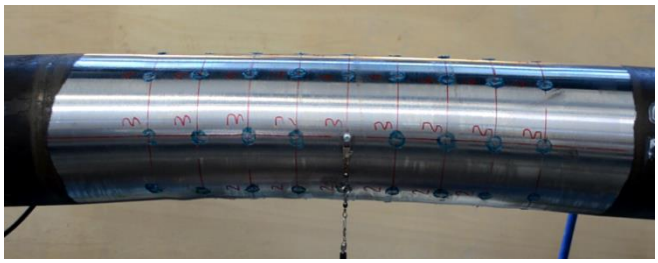

Figure 13: Initial uniform wrinkling during monotonic bending; SP8b specimen.

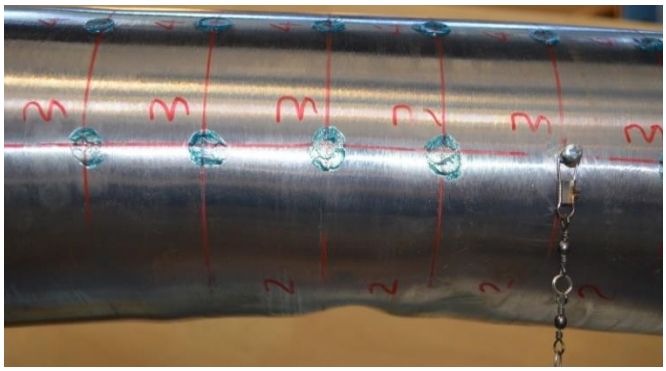

Figure 14: Localization of wrinkling, buckle development during monotonic bending; SP8b specimen

(a)

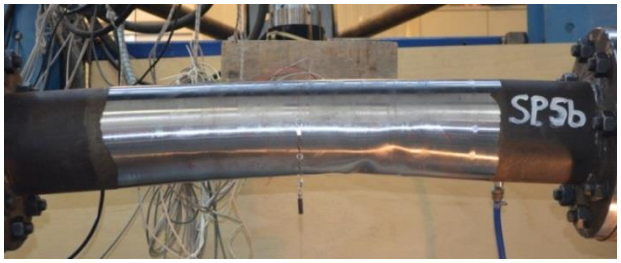

(b)

(c)

Figure 15: Buckled specimens (a) SP3b, (b) SP5b and (c) SP6b buckled specimens.

In all specimens, local buckle is developed after the formation of uniform wrinkles in the compression side of the pipe specimen (Figure 13). With increasing bending load, compressive strains also increase, resulting in the localization of damage, producing a non-symmetric buckle (Figure 14).

The final buckled shapes of the specimens at the end of loading application before the application of cyclic bending are shown in Figure 15 and Figure 16. Specimen SP3b buckled at the edge of the reduced-thickness (machined) region, close to the transition zone (Figure 15a and Figure 16a). On the other hand, the other specimens buckled near the mid-span of the machined thickness zone.

In particular, Figure 15d shows that specimen SP4b buckled almost exactly at the middle cross section. For each case of pipe specimens, the buckling pattern consisted of a diamond-type shape with one major buckle and two minor buckles on each side of the bending plane, as shown clearly in Figure 16b.

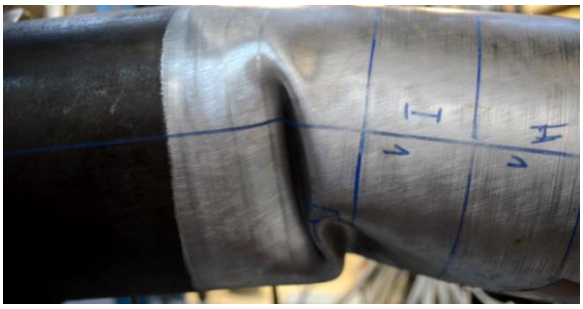

(a)

(b)

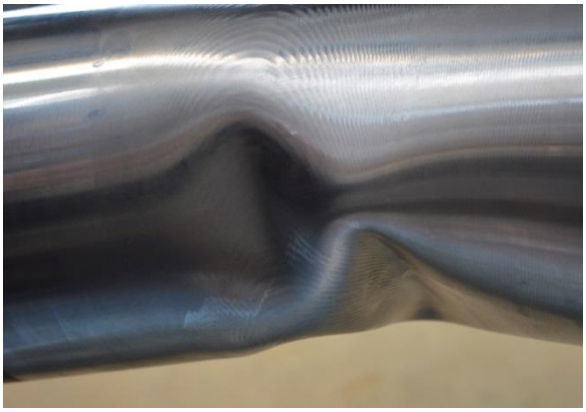

(c)

Figure 16: Detail of the non-symmetric buckle for (a) SP3b, (b) SP4b and (c) SP7b specimen.

Cyclic testing results on buckled specimens

After the formation of the buckled pattern, specimens SP3b-SP6b are subjected to cyclic loading via stroke displacement control conditions (Δu equal to about 10mm) until failure due to low-cycle fatigue. Table 2 summarizes the results on buckled specimens under consideration for both buckle development and cyclic loading. The loading sequence applied in specimens SP3b- SP6b (monotonic and cyclic) is presented in Figure 7.

Moreover, prior to cyclic testing, one tri-axial strain gauge has been installed on the critical region where a crack is most likely to occur (Figure 17). Based on previous experience [11] this location is the ridge of the most folded buckle. Local strain variations during cyclic loading are measured and the corresponding hysteresis loops are shown in Figure 18. It is observed that the hysteresis loops grow wider resulting in accumulation of local strains and, eventually, in fatigue cracking. Furthermore, axial strain values appear to be larger than hoop values. More specifically, with the application of a constant amplitude of stroke displacement variation (Δu) equal to 10mm, an increase of the local axial strain variations ($\Delta\varepsilon_x$) is observed initiating from values of 0.02% increasing up to 1.6% at failure. This, also, explains the fact that, upon cyclic loading, the cracks were propagated along the hoop direction perpendicular to the pipe axis. It is also observed from Figure 17 and Figure 18, that despite the fact that the majority of specimens have been excessively distorted, they have shown a remarkable strength against cyclic loading and failed under significant number of cycles.

The crack locations of the buckled specimens (SP4b-SP6b), subjected to cyclic bending, are presented in Figure 19. In SP5b and SP6b specimens, the crack initiated at the location where the tri-axial strain gauge has been placed before the cyclic loading stage. The crack propagated through the hoop strain gauge destroying the gauge (Figure 19b& c).

Table 2: Experimental results on buckled specimen subjected to cyclic bending

	1st Stage: Buckling Development				**2nd Stage: Cyclic Loading**	
Buckled Specimens	P_m (kN)	P_b/P_m	δ_m (mm)	$\delta_b-\delta_m$ (mm)	Δu (mm)	Nf_{tot}
SP3b	80.59	0.50	17.8	54.5	10	830
SP4b	66.67	0.50	15.2	43.8	10	590
SP5b	79.4	0.75	30	6.4	10	920
SP6b	78.4	0.65	18.2	19.8	9	200

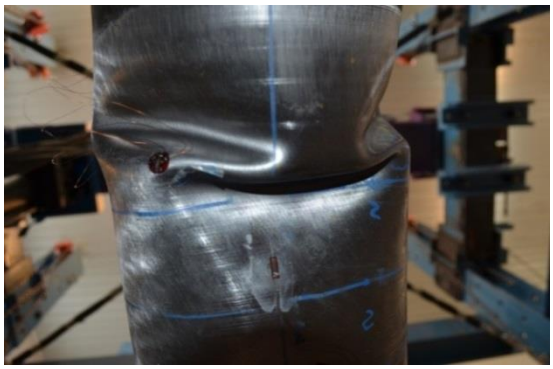
(a)

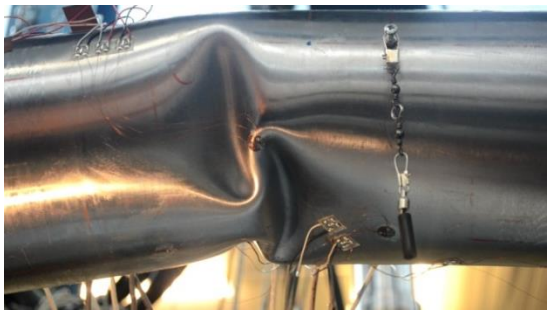
(b)

Figure 17: Tri-axial strain gauge installed on the critical region of the buckle for specimens (a) SP3b and (b) SP4b.

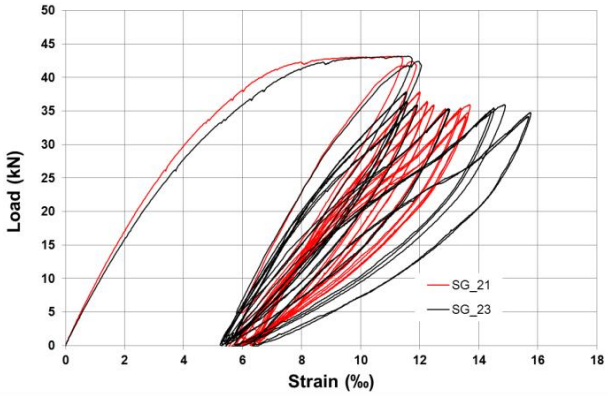

(a)

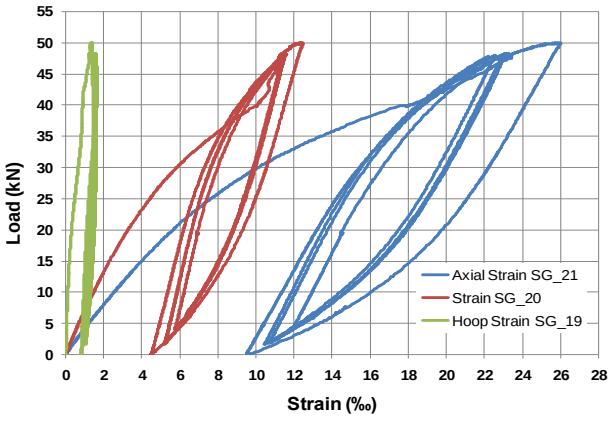

(b)

Figure 18: Strain variations measured on the buckle region, during cyclic loading for (a) SP3b and (b) SP6b specimens

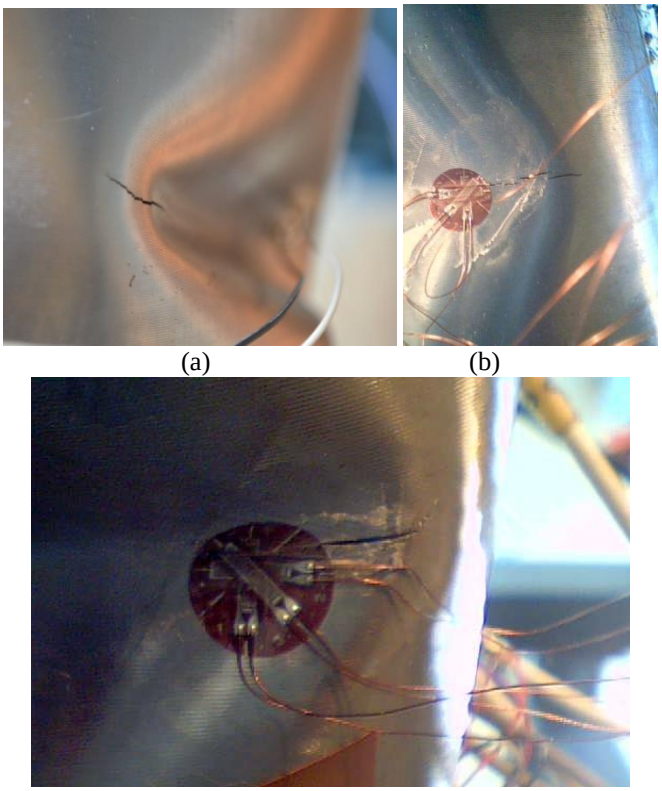

(a) (b)

(c)

Figure 19: Location of fatigue crack for 3 specimens; (a) SP4b and (b) SP5b and (c) SP6b.

Pressure tests results

Two (2) buckled specimens, namely SP8b and SP7b are tested under pressure loading. The results are summarized in Table 3. The buckled specimens are first subjected to pressure cycles with minimum and maximum pressure values equal to 0.92 MPa and 9.20 MPa, respectively which correspond to 72% of the nominal yield pressure $p_y = 2\sigma_y \frac{t}{D}$ equal to 12.8 MPa.

Specimen SP7b failed at 570 pressure cycles (Figure 20) with cracking and leakage at the buckle region. On the contrary, no failure or damage has been detected for SP8b specimen after 5000 pressure cycles. For this specimen, after 5000 pressure cycles, monotonically increasing pressure has been applied until burst. The specimen ruptured at 15.7 MPa away from the buckle area, as shown in Figure 21. The application of internal pressure resulted in a "smoothening" of the buckled area, as shown in Figure 21. It is interesting to notice that this value is somewhat lower than the theoretical value of burst pressure estimated from the following simplified formula $\sigma_b = 2\sigma_{UTS} \frac{t}{D}$, where σ_{UTS} is the ultimate tensile stress (σ_b=19.5MPa). This result shows that the presence of a smooth buckle on the pipe wall has a rather small effect on the burst capacity of the pipe.

Table 3.: Pressure loading of buckled specimens

	1st Stage Buckling		2nd Stage: Cyclic Pressure		
Buckled Specimens	P_m (kN)	Pb/Pm	ΔP (Mpa)	N	P_{burst} (MPa)
SP7b	89.25	0.50	8.3	570	--
SP8b	91.40	0.75	8.3	5000	15.7

Figure 20: Leakage of specimen SP7b due to cyclic internal pressure; wall rupture location at the buckle location.

Figure 21: Rupture of SP8b specimen, away from the buckled area

FINITE ELEMENT SIMULATION

Finite element tools are employed to simulate the development of buckling and the response of the buckled pipes under cyclic bending and pressure and provide an efficient tool for buckled pipeline assessment. The simulations are conducted with finite element program ABAQUS/ Standard. Nonlinear finite element models are developed, capable of describing large displacements and strains, as well as inelastic effects in a rigorous manner.

The central (machined) part of the pipe specimens simulated with four-node reduced-integration shell elements (S4R). Those elements have shown to perform very well in

nonlinear analysis problems of relatively thick-walled steel cylinders involving large inelastic deformations and buckling.

The remaining part of the tube specimen is simulated with appropriate beam elements of cross-sectional and material properties. Similarly, beam elements are employed for the stiff pipes with ∅197.3/10 stiff pipes. Following the experimental procedure, loading is applied at two points of the stiff pipes, corresponding to the locations of wooden grips. The general view of the finite element model is shown Figure 22.

To describe inelastic material behavior of the pipe specimens, a J_2 (von Mises) flow plasticity model with isotropic hardening is employed, calibrated through the uniaxial tensile stress-strain curve of the material. The use of this plasticity model may be criticized in the sense that it might not be capable of describing the cyclic response of steel material including the Bauschinger effect. The implementation of a more-elaborate cyclic plasticity model is under development, but it is out of the scope of the present work

Monotonic bending of pipes

The shape of the deformed finite element model is shown in Figure 23. Following the experimental procedure, local buckling occurs under 4-point bending loading via displacement control conditions. Three values for buckle levels are considered in this numerical study. As described previously, these levels correspond to values of P_b/P_m equal to 50, 65% and 75%. A typical buckle profile after monotonic bending is shown in Figure 23. Moreover, force versus displacement diagrams are compared well with the experimental curves as shown, indicatively, for specimens SP4b, SP7b and SP8b in Figure 24. The displacement values of the tests, correspond to the average movement recorded with the LVDTs placed at the two wooden hinges prior to monotonic testing.

The distribution of axial strains ε_x at the critical region of SP7b specimen is shown in Figure 25 after unloading and prior to cyclic testing.

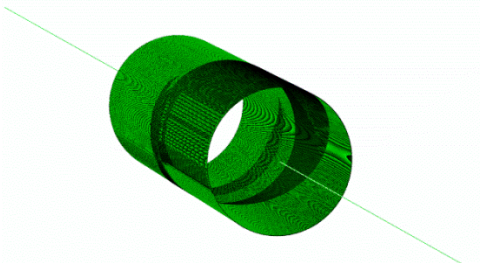

Figure 22: General view of the finite element model.

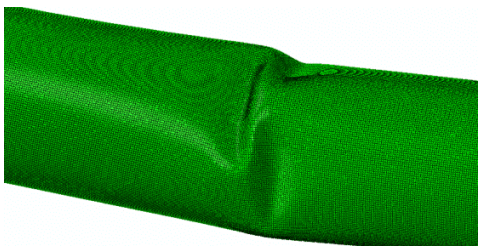

Figure 23: Deformed geometry of the pipe after buckling

Cyclic bending of buckled pipes

Following buckling, cyclic bending of the buckled pipe is simulated, similar to the experimental procedure. During the numerical simulation, cyclic bending of the specimens is performed until the deformation stages followed during the experimental procedure. At each stage, a total of 10 cycles is performed numerically, and the corresponding range of maximum local strains in the longitudinal direction with respect to the pipe axis is measured, as depicted in Table 4. The evolution of the maximum hoop and axial strains derived from the inner and outer pipe surface is shown in Figure 26 for specimen SP5b during cyclic bending.

Based on the values of local strain range, it is possible to employ the fatigue curve of the pipe material, expressed by equation (1) to conduct a simplified fatigue analysis. Towards this purpose, Miner's rule is consider to define a damage factor D_f, as follows:

$$D_f = \sum_i \frac{n_i}{N_i} \tag{2}$$

where N_i is the number of cycles corresponding to $\Delta\varepsilon_{\max}$ obtained from the fatigue curve ($\Delta\varepsilon - N$) and n_i is the number of real cycles applied. Strains are measured at the outside surface. The results of this analysis are depicted in Table 3 for three specimens. Specimen SP3b is excluded because it did not buckle near the central pipe region. Except for the case of SP7b specimen, the values of the damage factor are close to 1, indicating a good correlation between test results and numerical analysis.

Furthermore the strain concentration factor (SNCF) was estimated for each specimen under consideration. This SNCF factor is defined as follows:

$$SNCF = \frac{\Delta\varepsilon_{max}}{\Delta\varepsilon_{nom}} \tag{3}$$

The value $\Delta\varepsilon_{\max}$ is the maximum local strain range in the axial direction at the critical region, and $\Delta\varepsilon_{nom}$ is the nominal strain range due to the applied loading, calculated through elementary mechanics of materials, considering the initial (intact) geometry of the tubular member. More specifically, for cyclic bending loading conditions, the corresponding strain concentration factor is computed in terms of the maximum strain variation in the longitudinal direction of the pipe, whereas for four-point bending, $\Delta\varepsilon_{nom}$ is calculated as follows:

$$\Delta\varepsilon_{nom} = \frac{2\alpha\Delta F}{E\pi D^2 t} \tag{4}$$

where ΔF is the range of total transverse load applied on the specimen, and α is the distance between the hinge support and the point of load application.

The values of strain concentration factor are shown in Table 4. The numerical results indicate that upon cyclic bending loading, the *SNCF* can obtain significant values (order of magnitude). This is attributed to the fact that in the buckled area, the pipe wall is quite distorted (Figure 23) and the cyclic loading is associated with severe folding and unfolding of the pipe wall. The calculated values of *SNCF* are consistent with those reported by Dama et al [8] for locally buckled pipes.

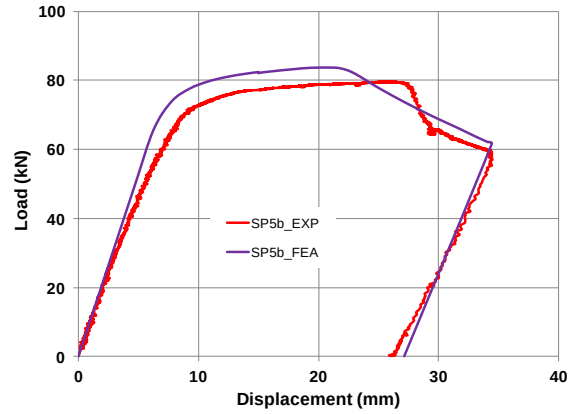

(a)

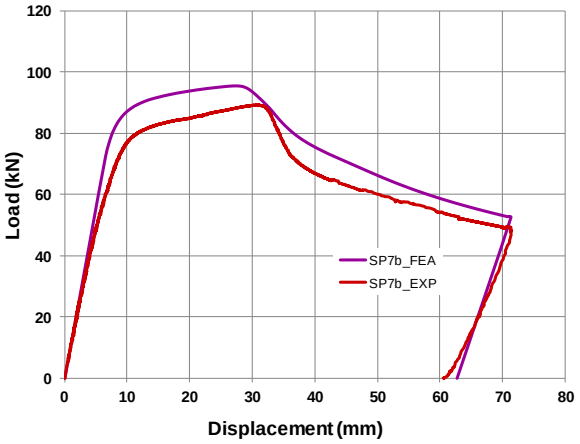

(b)

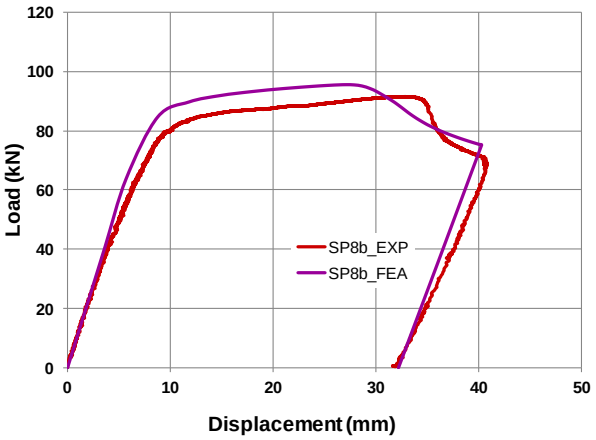

(c)

Figure 24: Load displacement curves for buckled specimens (a) SP4b, (b) SP7b and (c) SP8b.

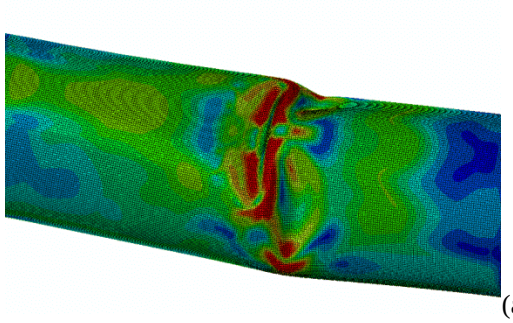

(a)

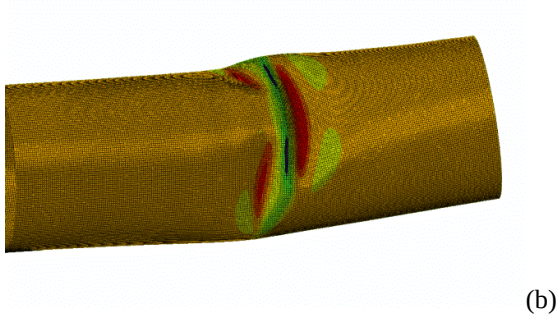

(b)

Figure 25: Distribution of (a) Von Mises stress and (b) axial (longitudinal) strain (ε_x) around the final buckle region; SP7b specimen

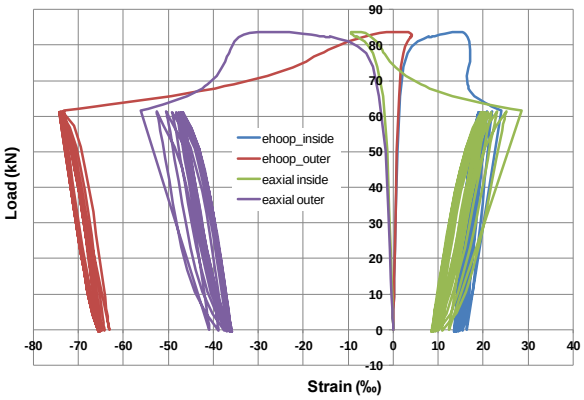

Figure 26**:** Strain values in the buckle region during monotonic and cyclic bending for specimen SP5b.

Table 4.: Fatigue analysis under cyclic bending

Specimen	Cycles applied N_i	$\Delta\varepsilon_{max}$ (%)	D_f	*SNCF*
SP4b	550	1.78	1.80	16.13
SP5b	920	1.42	1.19	8.63
SP6b	200	1.54	0.47	9.93

Simulation of pressure loading

Internal pressure is applied in the numerical model of the buckled specimens, following the test procedure of the two specimens (SP7b and SP8b). In particular, 10 pressure cycles of

Δp= 8.28 MPa are applied, while for SP8b specimen a combination of cyclic (10 pressure cycles) and monotonic pressure has been applied. The fatigue life for SP7b model and the burst pressure for SP8b specimen have been estimated. The SNCF values have been computed for both SP7b and SP8b specimens under cyclic pressure as shown in Table 4.

For cyclic internal pressure loading, the strain concentration factor is computed considering the maximum strain in the hoop direction. Furthermore, the corresponding nominal strain is computed from elementary mechanics of materials as follows:

$$\Delta\varepsilon_{nom} = \frac{D}{2t}\frac{\left(1-\nu^2\right)}{E}\Delta p \qquad (5)$$

where D and t are outer diameter and thickness of the pipe, respectively. E and ν are the Young's modulus of the pipe material and the Poisson's ratio, respectively, while Δp is the range of the imposed pressure which is constant for every cycle.

The results show that with increasing pressure, the buckled profile "smoothens" (Figure 27), the buckle depth is decreased, and there is a tendency of gradual flattening of the buckled area. Furthermore, for the range of cyclic pressure applied during the test on SP8b (Δp=8.3 MPa, with a maximum value of 9.2 MPa), the corresponding strain concentration factor *SNCF* is computed equal to 7.41 so that the local strain variation is 0.59% and the fatigue life of SP8b specimen can be estimated by Eq (1) equal to about 11,000 cycles. This verifies the fact that SP8b specimen is capable of sustaining 5,000 pressure cycles without failure or other damage, as observed experimentally. The maximum internal pressure obtained from the finite element analysis is equal to about P_{burst}= 20 MPa until convergence of solution is not possible due to excessive plastification of pipe wall. This pressure load is close to the analytical solution but greater than the burst pressure measured in the pressure test of SP8b. This is attributed to the fact that, around the region of rupture, pipe thickness value has been recorded equal to 2.2mm which is quite lower than the average value of 2.8mm. Concerning SP7b specimen, the SNCF computed numerically is significantly greater than the one calculated in the case of SP8b. This is due to the fact that, unlike SP8b specimen, the SP7b specimen's pipe wall was buckled excessively resulting in high local strain accumulation during cyclic pressure and, conclusively, SP7b sustained less pressure cycles.

CONCLUSIONS

Experimental investigation on six ∅165/3 X52 pipe specimens, machined from 6-inch-diameter pipes, has been conducted. The specimens have been buckled up to different buckle levels and subsequently subjected to cyclic bending or pressure. The buckled pipe specimens exhibited very good structural response under the application of cyclic loading. Numerical models have been developed to simulate the experimental procedure and compute the local strain variations during cyclic loading. Using this local strain information, a simplified method is employed to estimate the fatigue life of the pipe specimens using an appropriately defined damage factor providing good estimates for the specimen fatigue life.

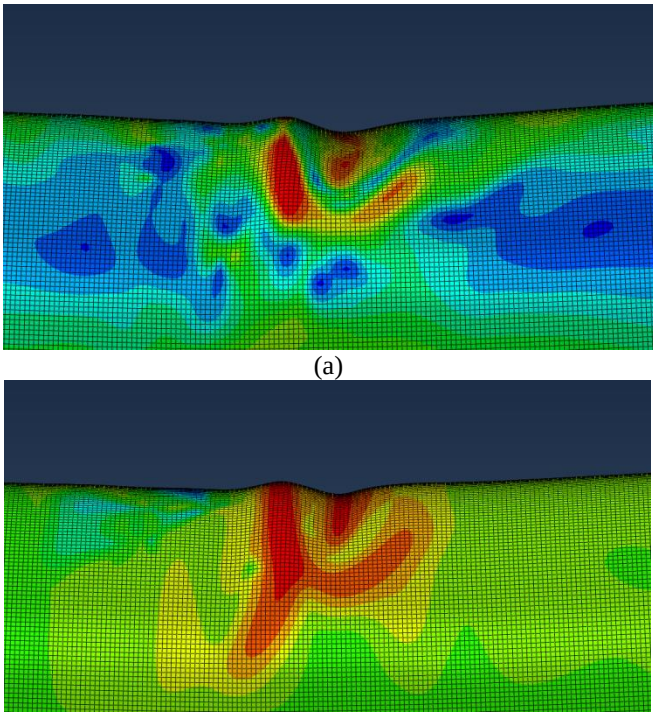

(a)

(b)

Figure 27**:** Buckle geometry: (a) before pressure application for SP8b and (b) after pressure application.

ACKNOWLEDGMENTS

This research has been co-financed by the European Union (European Social Fund – ESF) and Greek national funds through the Operational Program "Education and Lifelong Learning" of the National Strategic Reference Framework (NSRF) - Research Funding Program: Heracleitus II. Investing in knowledge society through the European Social Fund. The authors would like to thank EBETAM A.E. for providing the facilities for pressure testing, as well as Dr. Abilio M. P. de Jesus from FEUP for providing the material test data.

REFERENCES

[1] Doglione, R., and Firrao, D., 1998, "Structural Collapse Calculations of Old Pipelines," *International Journal of Fatigue*, **20** (2), pp. 161–168.

[2] Netto, T. A., Ferraz, U. S., and Estefen, S. F., 2005, "The Effect of Corrosion Defects on the Burst Pressure of Pipelines," *Journal of Constructional Steel Research*, **61** (8), pp. 1185–1204.

[3] American Petroleum Institute, *Fitness-for-Service*, API 579/ASME FFS-1, 2007

[4] Cosham, A., and Hopkins, P., 2004, "The Effect of Dents in Pipelines—Guidance in the Pipeline Defect Assessment Manual," *Int. J. Pressure Vessels Piping*, **81**, pp. 127–139.

[5] American Society of Mechanical Engineers, *Gas transmission and distribution piping systems*. ASME B31.8, 2007.

[6] Baker M., 2004, *Pipe Wrinkle Study,* Final Report to Department of Transportation, Research and Special Programs Administration Office of Pipeline Safety, OPS TT011.

[7] M. J. Rosenfeld, James D. Hart, Nasir Zulfiqar and Richard W. Gailing, "Development of Acceptance Criteria for Mild Ripples in Pipeline Field Bends" *4th International Pipeline Conference*, Sept. 29–Oct. 3, Calgary, Alberta, Canada, 2002.

[8] Dama, E., Karamanos, S. A. and Gresnigt, A. M., 2007, "Failure of Locally Buckled Pipelines.", *ASME Journal of Pressure Vessel Technology,***129**, pp. 272-279.

[9] Das, S., Cheng, J. J. R., Murray, D. W., 2007, "Prediction of the fracture life of a wrinkled steel pipe subject to low cycle fatigue load", *Canadian Journal of Civil Engineering*, **34** (9), pp. 1131-1139.

[10] Pournara, A. E. Karamanos, S. A., Papatheocharis, T. and Perdikaris, P. C., "Structural integrity of steel hydrocarbon pipelines with local wall distortions", *10th International Pipeline Conference*, ASME, IPC2014-33210, Calgary, Canada, 2014.

[11] Pournara, A. E. and Karamanos, S. A., 2012, "Structural integrity of steel hydrocarbon pipelines with local wall distortions", *Pressure Vessel and Piping Conference*, ASME, PVP2012-78131, Toronto, Canada

[12] American Petroleum Institute, *Specification for Line Pipe*, API-5L, 43th edition, 2004.

[13] Fernandes A.A. (coordinator), *Ultra Low Cycle Fatigue of steel under high-strain loading conditions*, 3rd Annual Progress Reportof ULCF-RFCS Project, Porto, 2013

